

Two-pathway four-state kinetic model of thioredoxin-catalyzed reduction of single forced disulfide bonds

Xiaochuan Xue,¹ Linchen Gong,¹ Fei Liu,^{1,*} and Zhong-can Ou-Yang^{1,2}

¹Center for Advanced Study, Tsinghua University, Beijing 100084, China

²Institute of Theoretical Physics, The Chinese Academy of Sciences, P.O. Box 2735 Beijing 100080, China

(Received 9 December 2007; published 20 May 2008)

Recent single-molecule experiments found that the thioredoxin-catalyzed reduction of individual disulfide bonds placed under a stretching mechanical force has distinct characteristics: the reduction rate of human thioredoxin monotonically decreases with the force, while the rate of *E. coli* thioredoxin first decreases and then increases as the force goes beyond a certain threshold. In this work, we present a force-dependent two-pathway four-state model to uniformly quantify these intriguing observations. Although our model is indistinguishable from the previous two-pathway three-state model in predicting the mean reduction rate, the distributions of dwell times of the two models are significantly distinctive. The very recent experiment favors our model.

DOI: 10.1103/PhysRevE.77.050903

PACS number(s): 87.15.ad, 82.37.Rs, 87.14.ej, 82.20.Uv

INTRODUCTION

The single molecule manipulation technique provides a novel approach to investigate biochemical and biophysical processes [1,2]. Compared with traditional bulk experiments, this approach not only allows for the direct application of force on single molecules of interest, but also can record the whole dynamic processes in real time. Many intriguing and even counterintuitive biomolecular characteristics have been revealed [3–5]. One of the recent illustrations is the study of thioredoxin- (Trx-) catalyzed reduction of single disulfide bonds placed under a constant stretching force [6,7]. Trx is an enzyme found in nearly all known organisms. It plays a critical role in disulfide bond reduction, maintenance of redox homeostasis, anti-apoptotic activity, and signaling [8]. Because the response of Trx in regulating the redox state in an organism could depend on conditions of mechanical stress [9], single molecule manipulation could be a direct method in understanding its enzymatic mechanism. The experiments found that the reduction rate of *E. coli* Trx does not depend monotonically on the mechanical force exerting on the disulfide bond; instead, the rate first decreases and then increases when force increases beyond a certain threshold. However, the reduction rate of human Trx (a homologue of the *E. coli* Trx) monotonically decreases with force. Interestingly, both types of mechanical responses of the Trxs are in contrast to the response of dithiothreitol (DTT), a simple chemical reducing agent, in which the rate is uniformly accelerated by force [10].

The Trx-catalyzed reduction of disulfide bonds has been studied in bulk solution [8,11,12]. The catalysis is thought to proceed through a substitution nucleophilic bimolecular (S_N2) reaction [8,13]. However, the reduction of a single disulfide bond under a stretching force is entirely new. To elucidate the distinct force dependence of the thioredoxin catalysis, Wiita *et al.* proposed a two-pathway three-state (TPTS) model [6]. One pathway is described as a Michaelis-Menten-like reaction [14] with a force-decelerated catalytic

rate. The other is simply a second-order reaction with a force-accelerated rate. This model could fit the mean reduction rates well. Under their theoretical frame, however, it is impossible to account for the latest experiment done by the same group [7]. The experiment found that the probability distribution of dwell times of the Trx-catalyzed reduction was double-exponential decay instead of monoexponential decay predicted by the TPTS model. Based on the existing knowledge about disulfide bond reduction and inspired by the molecular-dynamics simulation [6], in this Rapid Communication we present an alternative two-pathway four-state (TPFS) model to understand the forced reduction of disulfide bonds in quantitative and qualitative ways.

MODEL

The physical picture of our model is as follows. Trx has several discrete pathways for the thiol/disulfide exchange reactions with distinct catalytic rates [15]. These pathways can interconvert each other. Under a mechanical stretching force, the disulfide bond is initially fluctuating in thermal equilibrium. Upon binding with a Trx and selecting one of the pathways, the disulfide bond either unbinds from the enzyme and reforms a “free” bond again, or a thiol/disulfide exchange reaction occurs along the same pathway, which also indicates the break in the original disulfide bond, or it moves to one of the neighboring pathways. In addition to modulating the thermal fluctuation of the initial disulfide bond and interconversion rates between pathways, the force also accelerates the thiol/disulfide exchange reaction rates by lengthening the bond. Figure 1(a) is the simplest reaction scheme of the picture on which we focus in this work. This scheme includes two pathways and four states: two of them are the “free” bonds, and the others are the substrate-enzyme complexes.

According to the reaction scheme, the probability for the single disulfide bond to have a particular state at time t , $p_{S_i}(t)$, and $p_{ES_i}(t)$, $i=1,2$, can be obtained by solving linear differential equations. We write them into a matrix form,

$$\frac{d\mathbf{p}(t)}{dt} = \mathbf{Q} \cdot \mathbf{p}(t), \quad (1)$$

where $\mathbf{p}(t) = [p_{S1}(t), p_{S2}(t), p_{ES1}(t), p_{ES2}(t)]^T$, and the matrix \mathbf{Q} is

*liufei@tsinghua.edu.cn

$$\begin{pmatrix} -[\alpha_+(f) + k_{11}[\text{Trx}]] & \alpha_-(f) & k_{-11}[\text{Trx}] & 0 \\ \alpha_+(f) & -[\alpha_-(f) + k_{12}[\text{Trx}]] & 0 & k_{-12}[\text{Trx}] \\ k_{11} & 0 & -[\beta_+(f) + k_{-11} + k_{21}(f)] & \beta_-(f) \\ 0 & k_{12} & \beta_+(f) & -[\beta_-(f) + k_{-12} + k_{22}(f)] \end{pmatrix} \quad (2)$$

with the force-dependent interconversion rates $\alpha_{\pm}(f)$ and $\beta_{\pm}(f)$, the binding and unbinding rates k_{1i} and k_{-1i} , the force-accelerated reduction rates $k_{2i}(f)$, and the enzyme concentration $[\text{Trx}]$. Here we have assumed the force does not apparently affect the binding or unbinding rates. Because the disulfide bond under the stretching force is in thermal equilibrium before binding with the enzyme, which is usually satisfied in the single molecule experiment, the initial condition of Eq. (1) is

$$\mathbf{p}_0 = [p_0^1(f), p_0^2(f), 0, 0]^T = \left[\frac{\alpha_-(f)}{\alpha_+(f) + \alpha_-(f)}, \frac{\alpha_+(f)}{\alpha_+(f) + \alpha_-(f)}, 0, 0 \right]^T. \quad (3)$$

Hence, the quantities measured in the experiment, including the distribution of dwell times and the mean rate of the reduction, are calculated by $f(t) = \sum_{i=1}^2 k_{2i}(f) p_{\text{ES}_i}(t)$ and $v^{-1}(f) = \langle t \rangle = \int_0^{\infty} t f(t) dt$, respectively.

To compare with the experimental data, we still need the formulas of the force-dependent rates. Here we employ the widely used Bell expression [16]. Hence, the interconversion rates $\alpha_{\pm}(f) = \alpha_{\pm}^0 \exp(\pm \beta f d_{\pm})$ and $k_{2i}(f) = k_{2i}^0 \exp(\beta f x_i)$,

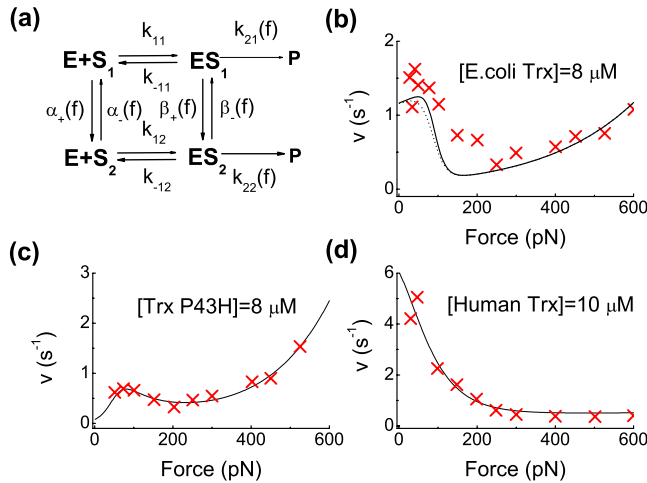


FIG. 1. (Color online) (a) The reaction scheme of our model. S_i , $i=1,2$, are states of the substrate disulfide bond, E is the enzyme Trx, and ES_i are the substrate-enzyme complexes occupying distinct reaction pathways. P indicates the break in of the disulfide bond. All involved reaction rates are denoted in the figure. (b)–(d) The mean reduction rates of the disulfide bond versus the applied force for WT E.coli Trx (b), Trx P43H (c), and human TRX (d). The red crosses are the experimental data from Ref. [6]. The black solid lines are directly calculated by our model. The dot line in (b) is calculated by Eq. (7).

where α_{\pm}^0 and k_{2i}^0 are the intrinsic rates at zero force, the positive x_i and d_{\pm} are the distances to the transition states, and $\beta^{-1} = k_B T$, where k_B is Boltzmann's constant and T is absolute temperature. We also set $k_{11} = k_{12} \equiv k_1$, $k_{-11} = k_{-12} \equiv k_{-1}$, and $\alpha_{\pm}(f) = \beta_{\pm}(f)$ to simplify the model. For any given kinetic parameters, the linear differential Eq. (1) can be readily solved by determining the eigenvalues and eigenvectors of the matrix \mathbf{Q} numerically.

RESULTS AND DISCUSSION

We first use the model to fit the experimental data, which include the mean reduction rates for E. coli Trx, Trx P43H, and Human Trx versus the applied mechanical force [6], and the distribution of dwell times of E. coli Trx at force 100 pN [7]. The results are shown in Figs. 1(b)–1(d) and 2, respectively, and Table I lists the fitting parameters. We see that, by choosing suitable values, our model can well fit the data. Particularly, our model can simultaneously account for the mean rate and the distribution of dwell times of the case of E. coli Trx with the same parameters [18]. We also plot the distribution predicted by the TPTS model [6,19] in Fig. 2. Although this previous model can fit the mean reduction rates, its prediction about the distribution of dwell times fails in that the distribution is always monoexponential.

After carefully checking the parameters in Table I, we find that, under the experimental conditions [6,7], the physi-

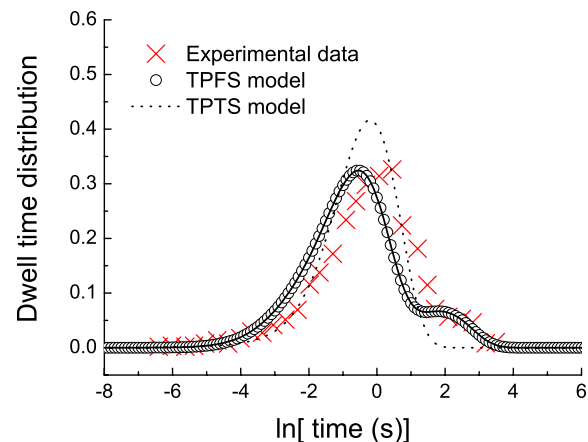


FIG. 2. (Color online) The distributions of dwell times of the E. coli Trx-catalyzed reduction of single disulfide bonds under force 100 pN and $[\text{Trx}] = 12 \mu\text{M}$. The red crosses are the data from Ref. [7]. The circles are directly calculated by Eq. (1), the solid line is calculated by Eq. (6), and the distribution given by the TPTS is also shown by the dotted line for comparison [19]. We plot the distributions versus the logarithm of the dwell times [7,17] here.

TABLE I. The kinetic parameters used in our model. The units of the distances are Å, and except for k_1 ($\mu\text{M}^{-1} \text{s}^{-1}$), the units of the other rates are s^{-1} .

	α_+^0	α_-^0	d_+	d_-	k_1
E.coli Trx	2.9×10^{-4}	0.674	2	0.5	3
Trx P43H	5.4×10^{-3}	0.085	0.25	0.25	3
Human Trx	4.7×10^{-3}	0.096	0.3	0.3	3
	k_{-1}	k_{21}^0	k_{22}^0	x_1	x_2
E.coli Trx	32	2.85	0.193	0.08	0.18
Trx P43H	32	0.189	0.0945	2	0.28
Human Trx	32	60	1.05	0.5	0.01

cal process of the E. coli Trx-catalyzed reduction of a single disulfide bond under a stretching force may be relatively simple [20]. First let us see the force dependence of the mean reduction rate. When a small force is applied on the disulfide bond, due to $p_0^1 \approx 1$ and $\alpha_+, \beta_+ \approx 0$, the reduction reaction proceeds only along the first pathway, namely $f(t) \approx f_1(t)$ and $v(t) \approx v_1(f)$, where $f_1(t)$ and $v_1(f)$ are, respectively, the distribution of dwell times and the mean reduction rate of the first pathway, which are given by the following equations with $i=1$:

$$f_i(t) = \frac{k_1 k_{2i} [\text{Trx}]}{2\mathcal{A}_i} [\exp(\mathcal{A}_i + \mathcal{B}_i)t - \exp(\mathcal{B}_i - \mathcal{A}_i)t] \quad (4)$$

with $\mathcal{A}_i = [(k_1[\text{Trx}] + k_{-1} + k_{2i})^2/4 - k_1 k_{2i} [\text{Trx}]]^{1/2}$ and $\mathcal{B}_i = -(k_1[\text{Trx}] + k_{-1} + k_{2i})/2$, and

$$v_i(f) = \frac{1}{\langle t_i \rangle} = \frac{k_{2i} [\text{Trx}]}{[\text{Trx}] + K_i(f)} \quad (5)$$

with $K_i(f) = [k_{-1} + k_{2i}(f)]/k_1$. Because the catalytic rate k_{2i} is accelerated by the force, we see an increase of the mean reduction rate in Fig. 1(b) initially. When the force increases further, the interconversion rates $\alpha_+(f)$ and $\alpha_-(f)$ between S_i or ES_i become comparable (or $p_0^1 \sim p_0^2$) but are still far slower than the binding-unbinding rates and thiol/disulfide exchange reaction rates. In other words, the E. coli Trx-catalyzed reduction of the disulfide bond may proceed along the two pathways independently and comparably without apparent exchange in probability. This situation is very similar to the quasistatic limit discussed in Ref. [21]. Under this limit, the distribution of dwell times and the mean reduction rate can be approximated as

$$f(t) = \sum_{i=1}^2 p_0^i(f) f_i(t) \quad (6)$$

and

$$v^{-1}(f) = \sum_{i=1}^2 p_0^i(f) v_i(f)^{-1}. \quad (7)$$

They are indeed the weighted mean of the dwell time distribution and of the reciprocal reduction rate of the two pathways in Fig. 1(a), respectively. Because of smaller x_1 , the

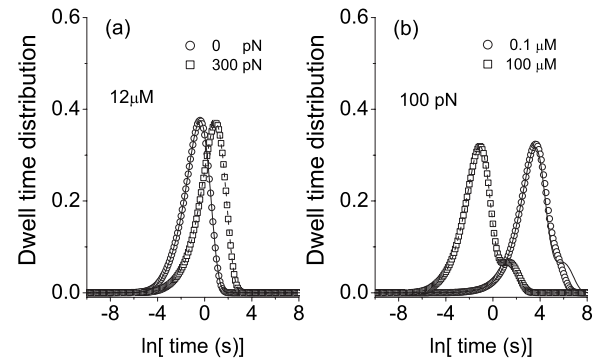


FIG. 3. Distributions of dwell times for the case of E. coli Trx under two forces with $[\text{Trx}] = 12 \mu\text{M}$ (a) and two concentrations with force 100 pN (b). The circles and squares are directly calculated by Eq. (1). The solid and dashed lines in (a) are obtained from the approximation of $f(t) \approx f_i(t)$, $i=1,2$ for force 0 and 300 pN, respectively. The solid and dashed lines in (b) are calculated by Eq. (6) at the concentrations 0.1 and 100 μM , respectively.

effect of the increase of k_{21} is counteracted by the significant decrease of the ratio of the first pathway. Although at the same time the role of the second pathway is rising and $k_{22}(f)$ is accelerated by the force, $k_{22}(f) < k_{12}(f)$ in a certain range of force still makes $v(f)$ decreasing. When the applied force is very large, we easily see that $p_0^2 \approx 1$ and $\alpha_-, \beta_- \approx 0$. Hence, the reaction only proceeds along the second pathway. Because the catalytic rate k_{22} exponentially increases with the force, we meet an increase of the mean rate again; see Fig. 2(b). Interestingly, according to Eqs. (6) and (7), the quasistatic limit includes the cases of the small and large force in mathematics. We calculate the mean reduction rate versus the force and the distribution of dwell times obtained under the quasistatic limit and show them in Figs. 1(b) and 2. We see that they agree well with the exact numerical calculations.

The above discussion also gives the main characteristics of the dwell time distribution of the reduction reaction. Given the experimental concentration of the E. coli Trx [6,7], we have shown $f(t) \approx f_i(t)$, $i=1,2$ for the small and large force, respectively. Apparently, these distributions are monoexponential decays in these two force regions. As an illustration, we compare these approximations with the exact calculations for the case of E. coli Trx at force 0 and 300 pN with the same parameters in Table I and $[\text{Trx}] = 12 \mu\text{M}$; see Fig. 3(a). The agreement confirms our expectation. In contrast, for an intermediate force, e.g., 100 pN in Ref. [7], the quasistatic approximation Eq. (6) clearly predicts that the distribution is double-exponential in that the reaction proceeds along the two pathways independently and comparably. Thus, we see double peaks in Fig. 2. We must point out that the quasistatic limit is not always satisfied for any force and concentration. Because this limit requires that the interconversion rates between the pathways be far slower than the other rates, we easily conclude that the higher the Trx concentration is, the more accurate the approximation is. The solid and dashed lines in Figs. 2 and 3(b) demonstrate this conclusion. However, it is no longer true for the lower concentration. Figure 3(b) gives such an example: for the case of the lower Trx concentration 0.1 μM and force 100 pN, the

distribution of dwell times directly calculated by Eq. (1) (the circles) is almost monoexponential, while the distribution calculated by the quasistatic approximation is double-exponential (the solid line). The lower concentration means that the substrate binding rate $k_1[\text{Trx}]$ may be comparable with the interconversion rates. Therefore, the significant exchange in probability between the two pathways make them blurred and results in a quasi-mono-exponential distribution. Because the distribution of dwell times provides a stricter requirement for a model, the results shown in Fig. 3 could be viewed as criterions of the correctness of our model.

SUMMARY

We close this work by pointing out the differences between the TPTS and TPFS models. Both of the models are supported by the existing structural evidence. The molecular-dynamics simulation found the disulfide bond sampling a range of conformation in the Trx enzymes [6], and previous theoretical calculations [15] and the experiments [7] implied the possible existence of multiple transition states for disulfide bond reduction. However, the details of the two models are actually significantly different. First, both pathways in the TPFS model require a reversible binding of the disulfide bond to an enzyme, which is not required by the TPTS

model. Second, the TPTS model phenomenologically introduced a force-decelerated catalytic rate to account for the decrease of the reduction rate in a range of force. In contrast, the catalytic rates in our model are always force-accelerated by force lengthening the disulfide bond. The first difference can be seen by the distribution of dwell times. The TPTS model predicts $f(t) \approx k_{02}[\text{Trx}] + o(t)$ in the short-time region, where $k_{02} = \gamma_0 \exp(\beta f \Delta x_{02})$ with $\Delta x_{02} > 0$; we used the same symbols in Ref. [6]. In other words, $f(0)$ does not vanish and increases with the force exponentially. This is in contrast with our model, in which $f(0)$ always vanishes. Hence, by choosing smaller bin size (≤ 50 ms given by the parameters in Table I) of the histogram of the dwell times, the experiment should distinguish which mechanism is more plausible. Compared to the first one, the second difference is subtle. We would need new single molecule experiments or molecular modeling to distinguish them.

ACKNOWLEDGMENTS

We are grateful to the referee for informing us of the new experimental result regarding the distribution of dwell times of the reduction reaction. This work was supported in part by Tsinghua Basic Research Foundation and by the National Science Foundation of China under Grant No. 10704045.

-
- [1] C. Bustamante, Y. R. Chemla, N. R. Forde, and D. Izhaky, *Annu. Rev. Biochem.* **73**, 705 (2004).
- [2] W. E. Moerner, *Proc. Natl. Acad. Sci. U.S.A.* **104**, 12 596 (2007).
- [3] E. A. Abbondanzieri, W. J. Greenleaf, J. W. Shaevitz, R. Landick, and S. M. Block, *Nature (London)* **438**, 460 (2005).
- [4] H. Itoh, A. Takahashi, K. Adachi, H. Noji, R. Yasuda, M. Yoshida, and K. Kinoshita Jr., *Nature (London)* **427**, 465 (2004).
- [5] B. T. Marshall, M. Long, J. W. Piper, T. Yago, R. P. McEver, and C. Zhu, *Nature (London)* **423**, 190 (2003).
- [6] A. P. Wiita, R. Perez-Jimenez, K. A. Walther, F. Gräter, B. J. Berne, A. Holmgren, J. M. Sanchez-Ruiz, and J. M. Fernandez, *Nature (London)* **450**, 124 (2007).
- [7] R. Szoszkiewicz, S. R. K. Ainarapu, A. P. Wiita, R. Perez-Jimenez, J. M. Sanchez-Ruiz, and J. M. Fernandez, *Langmuir* **24**, 1356 (2008).
- [8] A. Holmgren, *Annu. Rev. Biochem.* **54**, 237 (1985).
- [9] T. M. Paravicini and R. M. Touyz, *Cardiovasc. Res.* **71**, 247 (2006).
- [10] A. P. Wiita, S. R. K. Ainarapu, H. H. Huang, and J. M. Fernandez, *Proc. Natl. Acad. Sci. U.S.A.* **103**, 7222 (2006).
- [11] A. Holmgren, *J. Biol. Chem.* **254**, 9113 (1979).
- [12] G. Krause, J. Lundstrom, J. L. Barea, C. Pueyo de la Cuesta, and A. Holmgren, *J. Biol. Chem.* **266**, 9494 (1991).
- [13] A. Holmgren, *Structure (London)* **3**, 239 (1995).
- [14] L. Michaelis and M. L. Menten, *Biochem. Z.* **49**, 333 (1913).
- [15] P. A. Fernandes and M. J. Ramos, *Chem.-Eur. J.* **10**, 257 (2004).
- [16] G. I. Bell, *Science* **200**, 618 (1978).
- [17] F. J. Sigworth and S. M. Sine, *Biophys. J.* **52**, 1047 (1987).
- [18] For the case of *E. coli* Trx, we did not find a set of parameters that can closely fit the mean reduction rate and the distribution of dwell times simultaneously. One possible reason is that the former was approximately obtained by fitting ensemble-average force-clamp traces with a single exponential [6]. A simple calculation based on the experimental distribution of dwell times shows that this approximation may overestimate the reduction rate. Because all data have some uncertainties, we choose the set of parameters in Table I, which is a compromise between the data of the mean reduction rate and the distribution of dwell times.
- [19] Although Wiita *et al.* [6] investigated the TPTS model numerically, the model in fact has an analytic solution. Both the distribution of dwell times and the mean reduction rate can be obtained analytically.
- [20] Without the distribution of dwell times, the TPFS model cannot uniquely determine the kinetic parameters for the cases of Trx P43H and human Trx. We do not consider them in this work.
- [21] R. Zwanzig, *Acc. Chem. Res.* **23**, 148 (1990).